FLOODING IN HIGHLY TECTONIZED REGIONS OF NOCTIS LABYRINTHUS, MARS. J. Alexis P. Rodriguez[1-3], V. C. Gulick[1,3], Rogelio Linares Santiago[4], Mario Zarroca Hernández[4], A. G. Fairén[5], V. R. Baker[6], T. Platz[2], J. S. Kargel[6], Yan Jianguo[7] and N. Glines[1,3]. [1]NASA ARC, MS 239-20, Moffett Field, CA, 94035 (Alexis.Rodriguez@nasa.gov), [2]PSI, Tucson, AZ, [3]SETI Institute, 189 Bernardo Avenue, Mountain View, CA 94043.[4] External Geodynamics and Hydrogeology Group, Department of Geology, Autonomous University of Barcelona, 08193 Bellaterra, Barcelona, Spain, [5]Centro de Astrobiología, 28850 Madrid, Spain, [6]Department of Hydrology & Water Resources, University of Arizona, Tucson, AZ. [7]State KeyLaboratory of Information Engineering in Surveying, Mapping and Remote Sensing, Wuhan University, 430070 Wuhan, China.

Noctis Labyrinthus [NL] consists of a vast network of troughs and pits connecting the Tharsis Montes and western Valles Marineris. Our mapping shows that the canyons of western NL (Fig. 1A) consist of closely-spaced pits and troughs with floors that range in elevation between ~6500 and ~4000 m (Fig. 1B). Canyon margins align with regional faults and grabens and show little evidence of lateral scarp retreat (Figs 1A, 2A and 2B) while their floors retain regional tectonic structures (e.g., Fig. 2B).

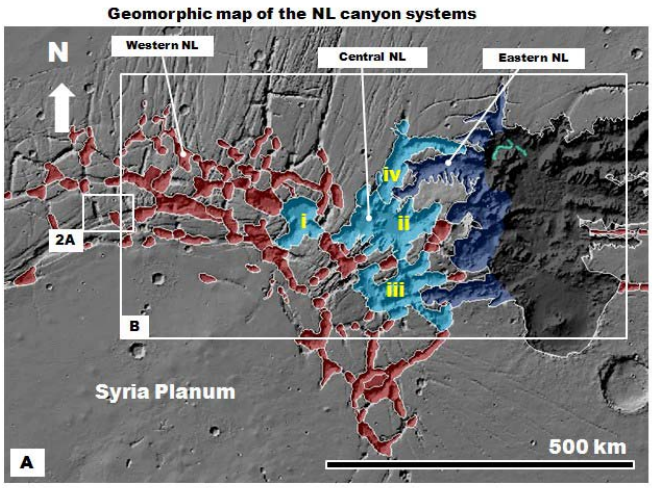

Fig. 1 (A) Geologic feature map showing the canyons of western (red), central (light blue), and eastern (dark blue) NL. White outlines = depression divides. MOLA shaded relief view centered at 7°20'S, 99°37'W. **(B)** Close-up view of elevation ranges, characterizing each mapped zones.

In contrast, canyons located in central NL have larger and deeper pits and troughs, with margins that are extensively modified by prominent alcoves (e.g., black arrow in Fig. 1B). These depressions are spatially integrated into four large enclosed basins (labels i, ii, iii, iv in Fig. 1A), with floors ranging in elevation between ~4000 to ~2000 m (Fig. 1B). The floors of basins (i) and (ii) are covered with materials that are bright in THEMIS night IR data (e.g., Fig. 3B), and suggest that these are likely bedrock [1]. These surfaces show a spectral signature consistent with a pyroxene-rich composition and have been interpreted as lava flows with a platy-ridged texture [2].

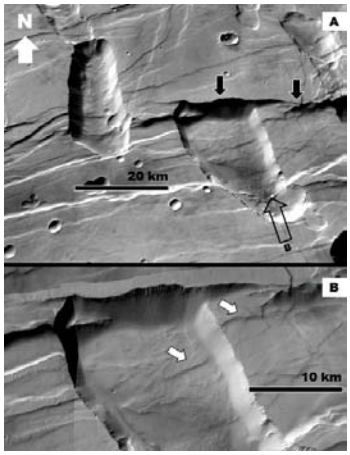

Fig. 2. (A) View of a trough and a contiguous graben in western NL, both bounded to the north by the same fault scarp (black arrows). Context and location in Figure 1A. **(B)** Close-up view on the trough floors reveals retention of pre-existing tectonic fabrics (white arrows). Perspective CTX views centered at 6°54'S, 104° 2'W.

Using impact crater counts Mangold et al. [2] also indicate that these surfaces were emplaced between ~50 and ~100 Ma (Late Amazonian), pointing to a potentially long history of resurfacing by volcanic processes. However, the identification of hydrated minerals, includes opal, gypsum, polyhydrated sulfates, and Al-clay deposits, and is consistent with these canyons experiencing multiple episodes of aqueous activity [3,4]. This recent hydrologic history remains poorly documented. Here, we propose that the contact between western and central NL (Fig. 1) represents the boundary of upper crustal zones of large-scale groundwater circulation, which led to extensive collapse and inundation within central NL.

The margin of basin (i) includes possible shoreline ridges (Fig. 3 C and D). On Earth, lake shorelines are generally recognized by the presence of wave-cut benches. However, in periglacial environments lake shorelines sometimes form ridges as sediments are pushed outwards during expansion/freezing cycles of the lake surface [5] (Fig. 3E). The basin's surface contains other landforms consistent with permafrost resurfacing; small domical structures that are locally modified by irregular quasi-circular summit pits (Fig.

4A). These structures might represent the remnants of pingos (Fig. 4B), which develop as upwelling groundwater interacts with permafrost forming domical features. Subsequent collapse of these features can produce summit pits. An alternative explanation is that Mars' low atmospheric pressure vaporized groundwater contained within pore space of shallow sediments, resulting in a pitted, hummocky surface. Mud volcanism (Fig. 4C) may have also resulted, possibly enhanced by seismic shaking and pressurization induced by the freezing upper zone, or by high thermal anomalies.

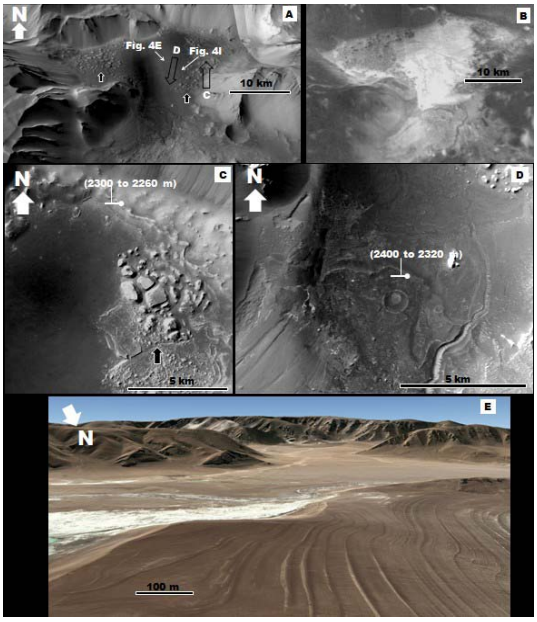

Fig. 3. (A) Perspective CTX view of basin i in Figure 1A. The black arrows show chaotic terrain materials embayed by a dark smooth deposit. Image centered at 6°51'S, 98°59'W. **(B)** THEMIS night IR view of basin floor shown in panel A showing that the deposit's surface exhibits high thermal inertia. **(C)** Close-up view on panel A showing the northeastern part of the basin, which exhibits chaotic terrains (black arrow) embayed by smooth floor deposits. **(D)** Close-up view on panel A showing the southern part of the basin, which exhibits a large channel extending into the basin's floor. The white arrows and pointers in panels C and D point to sets of marginal ridges, interpreted here as shoreline remnants. **(E)** Ridge-forming shorelines in a high elevation lake in the Tibettan plateau.

Irregular shallow depressions (Fig. 4D) may form as a consequence of thermokarst melting (Fig. 4E and F), or as a consequence of dissolution of surficial sediments. Polygonally patterned ground (Fig. 4G) forms within periglacial environments as a consequence of freeze-thaw processes or by expansion-contraction and ice condensation-sublimation cycles [6,7]. Polygons have formed in this region and have diameters ranging from a few up to ~20 meters (Fig. 4G). These diameters are consistent with those in terrestrial ice-rich permafrost regions [8]. However they are also consistent with those that occur in salt/playa lake environments [9] (Fig. 4 and I). An origin associated with tensile stresses during sediment desiccation is also possible, though the preservation of the resulting cracks seems to be much less probable.

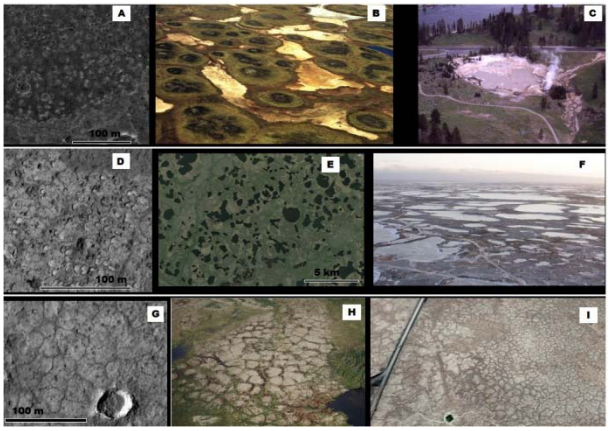

Fig. 4. (A) Lobate front within the deposit showing a surface marked by dense systems of pitted domes. Part of HiRISE view EPS_017465_1730. **(B,C)** Terrestrial analog pingos and mud volcanoes, respectively. **(D)** Thermokarst-like depressions within the basin's floor. HiRISE view ESP_019878_1730 centered at 6°52'S, 98°55'W. **(E, F)** Terrestrial analog thermokarst features. **(G)** Patterned ground within the basin's floor HiRISE view ESP_019878_1730 centered at 6°55'S, 98°53'W. **(H,I)** Terrestrial analog permafrost and playa polygonally patterned ground sites, respectively.

Here, we propose that the floor of basin (i) consists of indurated pyroxene-rich lacustrine sediments that have been modified by periglacial processes. Water at temperatures close to the freezing point would likely have hindered the alternation of these sediments to hydrated minerals such as phyllosilicates [10]. In summary, our observations are most consistent with extensive hydrologic resurfacing in central NL associated with groundwater circulation, erosion, and emergence below the ~ 4000 m elevation level.

References: [1] Christensen, P. R. et al. Science 300, 2056-2061 (2003). [2] Mangold, N. et al. Earth Planet Sc Lett 294, 440–450 (2009). [3] Weitz, C. M. et al., J. A. PSS 87, 130-145 (2013). [4] Weitz, C. M. & Bishop, J. L. Mars 8th Conf. abstract 1222. (2014). [5] Lee, J., Li, S. H. & Aitchison, J. C. Quat Geochronol 4, 335-343 (2009). [6] Costard, F. M. & Kargel , J. S. Icarus 114, 93-112 (1995). [7] Seibert, N. M. & Kargel, J. S. GRL 28, 899-902 (2001). [8] Levy, J., et al., JGR 114 (2009). [9] Hunt, C. B. & Wasburn, A. L. USGS Prof. Paper, 494-B, 104-133 (1966). [10] Fairén, A. G., et al. PSS 70, 126-133 (2012).

Acknowledgements: Funding provided by NASA's NPP program to J. Alexis P. Rodriguez and by MRO HiRISE Co-Investigator funds to V.C. Gulick. Funds for Alberto Fairén were provided by the European Research Council under the European Union's Seventh Framework Programme (FP7/2007-2013), ERC Grant agreement no. 307496.